Roman Kostecki, Heike Ebendorff-Heidepriem, Claire Davis, Grant McAdam, Tianyu Wang, and Tanya M. Monro
Fiber optic approach for detecting corrosion
Proceedings of SPIE: Sensors and Smart Structures Technologies for Civil, Mechanical, and Aerospace Systems, 2016 / Lynch, J.P. (ed./s), vol.9803, pp.98031I-1-98031I-14

DOI abstract link format:
http://dx.doi.org/10.1117/12.2219496

Fiber Optic Approach for Detecting Corrosion

Roman Kostecki[a,b], Heike Ebendorff-Heidepriem[a,b], Claire Davis[c], Grant McAdam[c], Tianyu Wang[b], and Tanya M. Monro[a,b,d]

[a]ARC Centre of Excellence for Nanoscale BioPhotonics, The University of Adelaide, Adelaide, SA 5005, Australia
[b]Institute for Photonics and Advanced Sensing and School of Physical Sciences, The University of Adelaide, Adelaide, SA 5005, Australia
[c]Defence Science and Technology Group, Fishermans Bend, Victoria, Australia
[d]University of South Australia, Adelaide, SA 5001, Australia

ABSTRACT

Corrosion is a multi-billion dollar problem faced by industry. The ability to monitor the hidden metallic structure of an aircraft for corrosion could result in greater availability of existing aircraft fleets. Silica exposed-core microstructured optical fiber sensors are inherently suited towards this application, as they are extremely lightweight, robust, and suitable both for distributed measurements and for embedding in otherwise inaccessible corrosion-prone areas. By functionalizing the fiber with chemosensors sensitive to corrosion by-products, we demonstrate in-situ kinetic measurements of accelerated corrosion in simulated aluminum aircraft joints.

Keywords: Corrosion, Sensors, Smart structures, Nondestructive evaluation, Structural health monitoring, Fiber optic sensors, Microstructured fibers, Nanostructure fabrication, Optical sensing and sensors, Thin film devices and applications.

1. INTRODUCTION

Corrosion remains a multi-billion dollar problem in industry.[1,2] An increasing recognition of the potential cost savings derived from early warning of corrosion problems has led to an increasing focus on corrosion monitoring as part of a preventive and predictive maintenance regime. The high acquisition costs associated with modern military and civilian aircraft coupled with tighter budgets has resulted in the need for greater utilization of existing aircraft fleets. Typically, military aircraft have a planned life-of-type of 25–30 years. In Australia, in many cases, almost twice this time has been achieved before the aircraft is retired.[3] For civilian aircraft flying today, approximately 20% are considered to be aging, and as that number increases so does the need for heightened fleet monitoring by airlines and manufacturers[5] combined with intense focus and surveillance of these activities by regulatory agencies.[6]

Send correspondence to Roman Kostecki: roman.kostecki@adelaide.edu.au

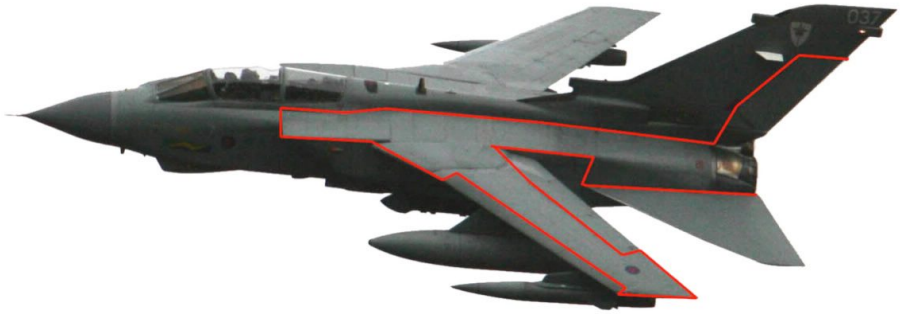

Figure 1: The concept of aircraft fitted with a distributed optical fiber sensor in ▮ – red, from Ref. 4.

Sensors and Smart Structures Technologies for Civil, Mechanical, and Aerospace Systems 2016, edited by Jerome P. Lynch, Proc. of SPIE Vol. 9803, 98031I · © 2016 SPIE
CCC code: 0277-786X/16/$18 · doi: 10.1117/12.2219496

With advancing aircraft age there is an increased possibility that protective coatings will break down or be damaged, resulting in exposure of the base material to the environment and an increased possibility of corrosion.[5] The operational loads on the structure also increase the possibility of structural fatigue damage, which constitutes one of the most significant safety concerns due to the potential for corrosion to reduce the fatigue life of the aircraft.[7] While attempts are made to prevent and reduce the effects of corrosion, in practice it is impossible to completely avoid. It is therefore essential that corrosion processes are monitored so that the inspection intervals are optimized and repair time and costs are minimized.

The detection of corrosion is particularly challenging in the sub-structure of an aircraft, such as lap joints, stiffeners and under sealant beads, since access to these areas usually requires time consuming and therefore costly disassembly.[3] Such areas are recognized as being particularly prone to corrosion, due to the possibility of creating a micro-environment within the crevices between the plates, accelerating the corrosion process.[7] Current non-destructive inspection methods, typically based on the use of a hand held ultrasonic probe, require a 5–10% section loss for corrosion to be reliably detected, at which stage the damage may be too severe to repair, and so the component often needs to be replaced.[3] Clearly a more proactive approach is needed to detect the initial onset of corrosion within these difficult to inspect areas.

Because corrosion can be very localized but can occur anywhere across a large structure, it is a broad area problem which requires a detection and/or monitoring system with the potential for distributed measurements, alerting the operator to the onset and location of corrosion. Optical fiber based sensors offer several inherent advantages when applied to structural platforms; they are immune to electro magnetic interference, easily networked, inherently suited to distributed sensing, and are typically in the order of only a few hundred microns in diameter making them very lightweight and suitable for embedment in inaccessible corrosion-prone areas. A number of fiber optic systems have been developed for single point corrosion monitoring, but only a few of these systems have exploited the capability of optical fibers for distributed measurements. Many of the aircraft fuselage components are fabricated from aluminum-based alloys, hence aluminium ions (Al^{3+}) are of particular interest because they are not only an indicator of the onset of corrosion,[3] but also have the potential to be an environmental hazard.[8] The concept of an aircraft fitted with a distributed optical fiber sensor is shown in Fig. 1.

2. PRINCIPLES AND BACKGROUND

Initial work on the fluorometric detection of Al^{3+} as an indicator of aluminum corrosion was conducted by the Australian Defence Science and Technology Group (DSTG), part of Australia's Department of Defence, in conjunction with Monash University in the early 2000s. These experiments focussed on the use of conventional large core multi-mode fibers (MMFs). As part of this research a range of different permeable polymer systems, doped with a compound that fluoresces in the presence of Al^{3+} were evaluated. The most promising of these, a flexible polyurethane the main constituent of which is a polyether,[3] was shown by McAdam *et al.* in 2005. The polymer was doped with a fluorescent compound, 8-HQ, which reacts with Al^{3+}. 8-HQ is an aromatic nitrogen compound characterized by a double-ring structure, containing a benzene fused to pyridine at two

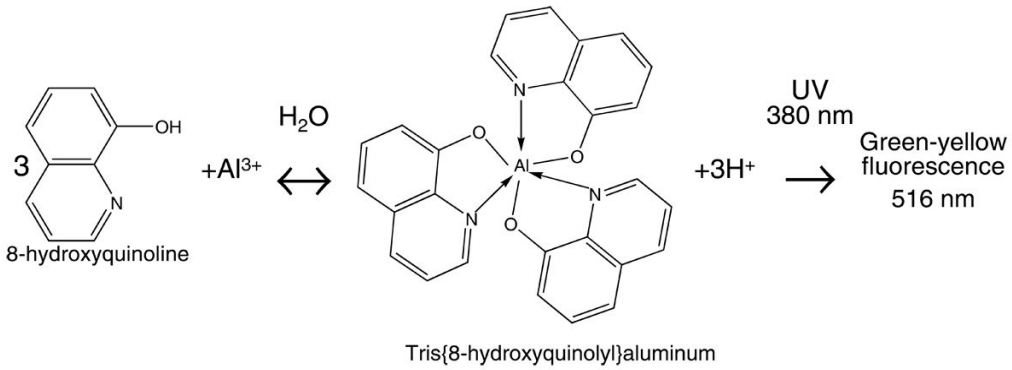

Figure 2: Reaction sequence for 8-HQ with Al^{3+} from Ref. 3.

adjacent carbon atoms, with the formula C_9H_7NO (Fig. 2(left)). This compound has a hydrogen atom that is replaceable by a metal, and gains its fluorescent nature by forming a dative bond between the metal and hetrocyclic nitrogen atom, enabling formation of a five-membered chelate ring with Al^{3+}. It is a bidentate ligand which forms a stable multi-ligand complex with Al^{3+}.[9] A 3^+ charge metal ion, as for the Al^{3+} case, forms a tris[8-hydroxyquinoline]metal(III), as shown in Fig. 2. The rigid octahedral complex that forms between three 8-HQ molecules and Al^{3+} fluoresces strongly at 516 nm (max) when excited by ultraviolet (UV) light in the range 360 to 390 nm,[10] although it has also been shown to work effectively when using a 405 nm excitation light source.[11]

The doped polymer was dip-coated onto the distal end of a MMF to create a sensing polymer bead at the fiber tip and placed into the channel of a simulated lap joint which was subjected to accelerated corrosion using a salt spray chamber. The measured back fluorescence from this optical fiber tip sensor increased as a function time, indicating an increasing presence of Al^{3+} due to progressing aluminum corrosion.[3] For this case, where the bead is attached to the end of an optical fiber, there are fewer physical constraints on the properties of the permeable coating used to contain the fluorescent species compared to a distributed sensor. Ideally, it would be preferable to create sensitivity to Al^{3+} by coating the fiber along the length, thus creating a distributed sensor rather than a local (point) sensor. In order to make distributed measurements the fraction of guided light propagating along the outside of the core needs to be accessed, which requires careful tailoring of the cladding refractive index and thickness to optimize the light/fluorophore interaction.

The concept of distributed detection of fluorescence from 8-HQ complex with Al^{3+} in solution was demonstrated by Sinchenko *et al.*[11] By using a large solid core (200 μm) MMF made from silica with the cladding removed, it was shown that optical time-domain reflectometry (OTDR) could be used to not only detect the presence of Al^{3+} in solution but also locate the position of this fluorescence 80 m along the fibers length. Figure 3(a) shows the setup, where photon counts were accumulated by time-gated electronics with a length resolution along the fiber of ~0.2 m. The signal detected is shown in Fig. 3(b), which represents the time domain response of the detection system when the de-clad fiber section was immersed in a 5×10^{-3} M solution of the 8-HQ–Al^{3+} complex. This experiment, described in detail in Ref. 11, demonstrated the that distributed fluorescence detection of cations, and in particular Al^{3+}, is possible. The power fraction (PF) of guided light propagating along the outside of the glass core was able to be used to excite the 8-HQ complex and the fraction of emitted florescence recaptured by the fiber core could be measured by time-gated electronics. However, using such a large core MMF meant that less than 0.1% of the total optical power propagates outside the core, making it impractical

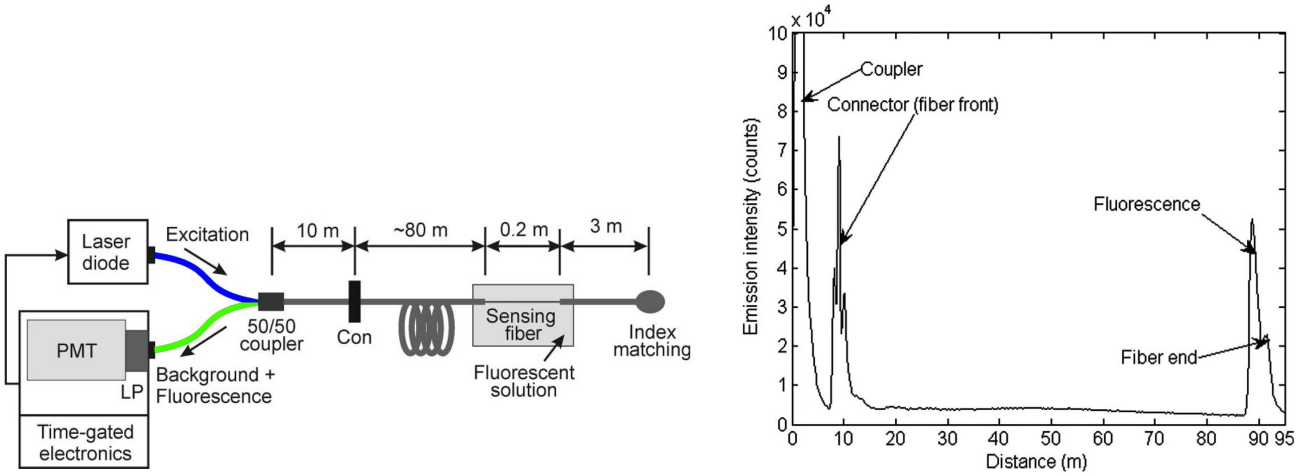

(a) (b)

Figure 3: (a) OTDR setup for distributed measurements of Al^{3+} (LP, long pass; Con, connector) in solution using a MMF silica fiber with 200 μm core; with which the (b) time of flight resolved fluorescence response of the 8-HQ complex within solution corresponds to detection position along the fiber.[11]

for applications requiring low detection limits.[12] Nevertheless, it is possible to increase this power fraction by reducing the core diameter.

Figure 4 shows a theoretical estimate[13] of the PF outside a circular silica core, for core diameters from 460 nm to 10 μm. The excitation and fluorescence wavelengths used for this study were 375 nm and 516 nm respectively, being the excitation and fluorescence wavelengths of the 8-HQ–Al^{3+} complex, and for the region surrounding the silica core a refractive index of water ($n = 1.33$) was used. As a first approximation, the coupled incident beam waist was set at the same diameter as the core, which is reasonable for micron scale (> 1 μm) core diameters. The total PF of all propagating modes excited by the incident beam as a function of the core diameter is shown by the red curve in Fig. 4(a). This PF curve shows that for core diameters less than 4 μm the fraction of power available for fluorophore excitation starts to significantly increase, being 0.3 and 2.1% at 4 and 2 μm diameters respectively. For core sizes below 1 μm in diameter there is another significant PF increase, where the calculated values are 2.8 and 17% at 1 μm and 460 nm diameters respectively. The corresponding fluorescence capture fraction (FCF) is shown by the blue curve in Fig. 4(a). The FCF is defined as the fraction of fluorescent photons that are coupled to the guided mode(s) of the fiber. Although the total PF was used to calculate the FCF, for simplicity only the FCF into the fundamental mode (HE11) of the fiber was considered for the special case of an attenuation-free fiber of infinite length. This FCF curve varies from a minimum of 1.1% to a maximum of 1.7%.

The intensity of fluorescence that is measured from the backward propagating modes of the fiber is the result of both the incident excitation power and the number of fluorescence photons recaptured. These quantities can be brought together to provide a better understanding of the overall performance of the sensor as a function of the core diameter by defining a figure of merit (FOM), FOM=(PF)·(FCF).[12] This FOM is shown in Fig. 4(b), where we observe an order of magnitude increase in sensor performance between the peaks at 8 and 2 μm, and no significant change in performance from 2 to 1 μm. Another factor, which will influence the FOM, is the fiber loss, which increases with smaller core diameters (and therefore greater PF) due to the increased scattering resulting from surface imperfections. Hence, the goal was to create a robust small core fiber which can be placed in situ and be capable of detecting the onset and monitor the progress of corrosion anywhere along its length within the aircraft fuselage.

While glass nano-wires,[14] as shown in Fig. 5(a), provide a way of producing centimeter scale lengths of small cores from conventional fibers, they are fragile and not practical for a distributed sensor needing lengths in the

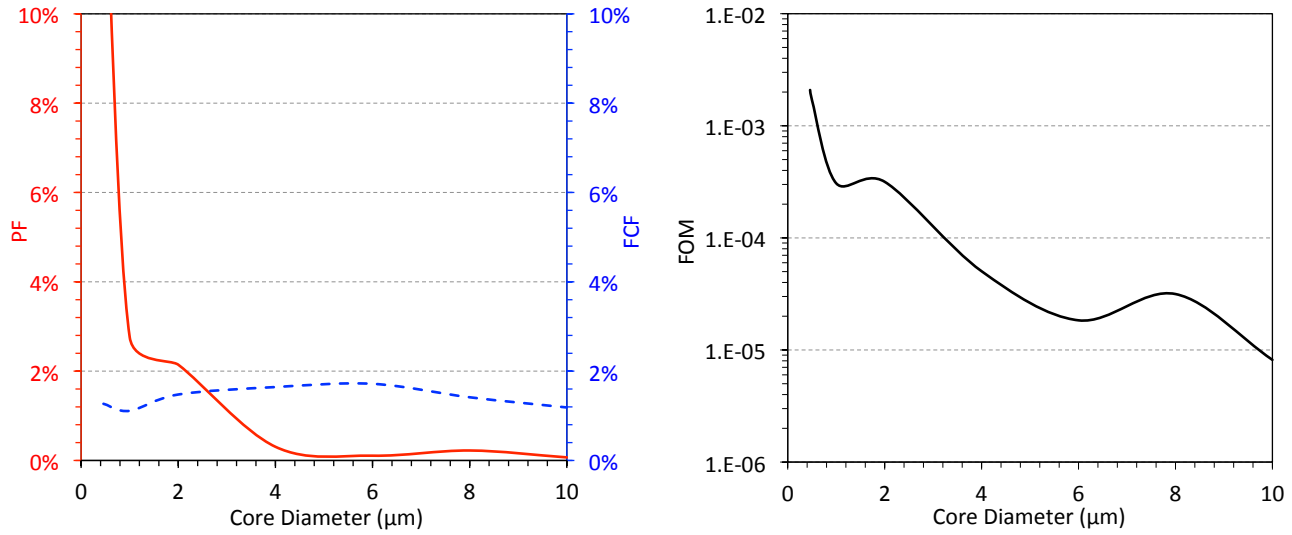

(a) (b)

Figure 4: (a) [▮ - Red solid line] Fraction of guided light power propagating outside a silica core as a function of core diameter assuming Gaussian beam excitation, and [▮ - Blue dashed line] the corresponding fluorescence capture fraction into the fundamental mode; and (b) the figure of merit as a combination of both.

order of hundreds of meters. On the other hand, a microstructured optical fiber (MOF)[15] provides a means for obtaining long lengths of uniform micrometre-nanometre scale suspended and protected cores. In particular, the suspended-core MOF (SC-MOF)[16] design, which consists of a small glass core suspended by thin struts inside voids within the fiber, have dramatically improved fluorescence-based fiber sensors by making use of the increased PF provided by the micrometer scale core size and therefore increased sensor performance.[12,17] Figure 5(b) shows a SC-MOF based on undoped high purity fused silica known as Heraeus Suprasil F300HQ silica (F300HQ), and Fig. 5(c) shows an enlargement of the core and holes region in the centre of the fiber, where the core of the fiber is the small triangular element in the centre of the image (highlighted by the green box), suspended on three thin struts.

While SC-MOFs have provided a highly sensitive sensing platform exploiting the significant fraction of guided power located within the holes,[12,19–24] the closed structure makes it impossible to use them for distributed sensing applications. To overcome this an exposed-core MOF (EC-MOF) geometry was developed to allow interaction of guided light with the surrounding medium along its length.[25,26] This was done by effectively opening up one of the voids within the preform before drawing to fiber. This method provides the ability to fabricate EC-MOFs hundreds of meters long with a fixed microstructured cross section. Warren-Smith showed that the EC-MOF has fast response and is capable of real-time sensing anywhere along the fiber length, making this type of fiber ideal for distributed sensing.[26] It was demonstrated that fluorescence emission coupled into the backward modes of a MOF core has higher efficiency compared to the forward modes.[13,27] This means that fluorescence measurements are enhanced when evaluating the back reflected signal, as shown by the schematic in Fig. 6. Warren-Smith also demonstrated fluorescence based distributed sensing by performing OTDR measurements using EC-MOFs.[28]

Fabrication of these small-core EC-MOFs was a significant milestone in the development of a distributed fiber optic corrosion sensor. For the first time, small core distributed fluorescence measurements became possible,[28] where the increased PF from the guided light propagating outside the small core could be accessed anywhere along its length whilst still being supported by the outside structure. Unfortunately, it was found that the Schott F2 soft glass (F2) material was not suitable for long term use and/or harsh environments,[26,29] where the loss and deterioration issues associated with the soft glass material precluded their long-term practical use under harsh conditions.[4] To produce a distributed fiber optic corrosion sensor capable of withstanding the intended harsh conditions, fiber materials other then soft glass were investigated. Both polymer and silica have material properties that made them attractive for optical fiber sensing applications.[30,31] Poly(methyl methacrylate) (PMMA) polymer optical fibers (POFs) have high elastic strain limits, high fracture toughness, and high flexibility in bending, and so initial work was performed to establish the suitability of polymer to create a robust optical fiber based distributed corrosion sensor. It was found that the high attenuation properties and difficulties with splicing, cleaving and coupling made small core size exposed-core POFs sensors challenging.[31–34]

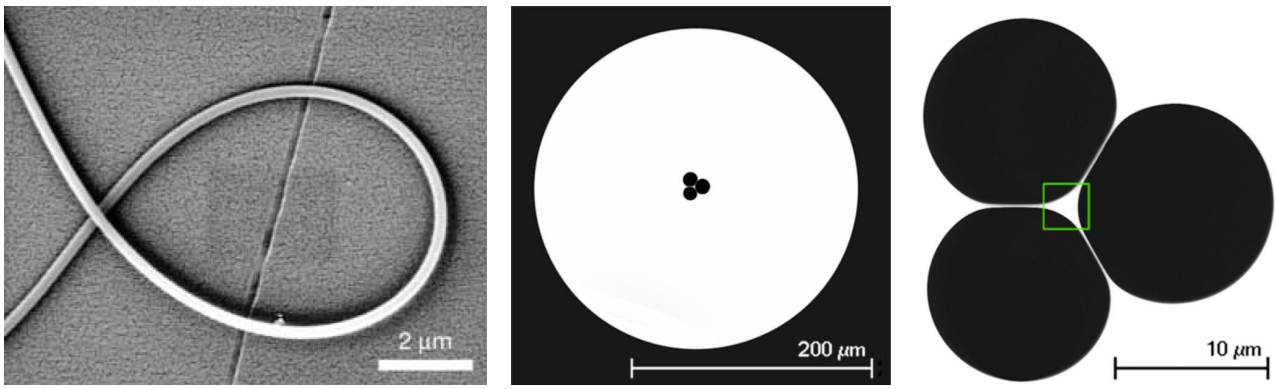

(a) (b) (c)

Figure 5: Scanning electron microscope (SEM) cross section images of (a) glass nano-wire from Ref. 14; (b) the silica SC-MOF (polymer coating removed) with an OD of 270 μm; and, (c) an enlarged image of the core and hole region, where the core is highlighted by the ▮ – green box, having an effective diameter of 1.7 μm.[18]

On the other hand, silica is known to be reliable under a range of processing conditions and applications, with relatively better mechanical and thermal stability compared to polymer or soft glass.[30] Highly homogeneous, high purity bulk material is commercially available, which has led to the development of low loss silica telecom fibers.[35] Silica has a relatively low refractive index, which can improve the sensitivity of evanescent field sensors, since reducing the index contrast (Δn) at the core-cladding boundary increases the PF.[12]

3. SILICA EXPOSED-CORE MICROSTRUCTURED OPTICAL FIBERS

As discussed in the previous section, the rationale behind producing silica EC-MOFs for long length distributed sensing of corrosion was to make a physically robust sensing element. The fabrication of a microstructured fiber with the core exposed along the whole length provides near-instantaneous measurements of fluorescence intensity while additionally allowing the opportunity for spatially distributed measurements along the length of the fiber through temporal detection methods such as OTDR.[26] High purity F300HQ fused silica was chosen because of its low hydroxide (OH^-) content and availability with tight geometric tolerances.[36] This material has high transmission in the UV–visible–near-infrared spectral range, making it suitable for a range of fluorophores. Unlike soft glass, the glass transition temperature of silica is high making it challenging to extrude, and since the EC-MOF are asymmetric, new fabrication methods needed to be established.

When fabricating structured optical fibers it is important to control the size and shape of the hole structure in a finished MOF. This is because when the MOF is drawn down to the typical 100–250 μm diameter from the typically 10–25 mm diameter preform, the structure experiences substantial external deformation under draw tension. Systematic experiments were performed and analytical equations worked out in order to understand how to reliably draw the EC-MOF geometry to optical fiber using silica.[37]

Figure 7(a) shows the geometry of an EC-MOF which was produced by drilling three holes in an equilateral triangle pattern and machining a slot along the length of one of the holes in an initial 20 mm diameter F300HQ silica rod.[38] This preform was then cleaned using acetone and water (ultra pure Milli-Q), then submersed in 70% nitric acid for 12 hours followed by a rinse with water and dried at 80°C. These methods expanded on a combination of work previously shown by Webb *et al.*[20] for fabricating a silica SC-MOF by drilling the preform, and Warren-Smith *et al.*[26] for cutting a thin slot into the side of the symmetric preform (soft glass) in order to expose the core region. The loss of this EC-MOF is shown in Fig. 7(b), with more then an order of magnitude less loss then the first silica EC-MOF we showed in Ref. 38. This relatively low loss has the potential to increase the OTDR distributed sensing range, where at 0.1–0.15 dB/m loss level the achievable distributed sensing range would be about 80 – 100 m at signal-to-noise ratio of 30.

The next step was to functionalize this silica EC-MOF into a sensing element for the detection of corrosion. Although the 8-HQ sensor molecules provide a method for fluorescence based Al^{3+} detection,[39] existing methods

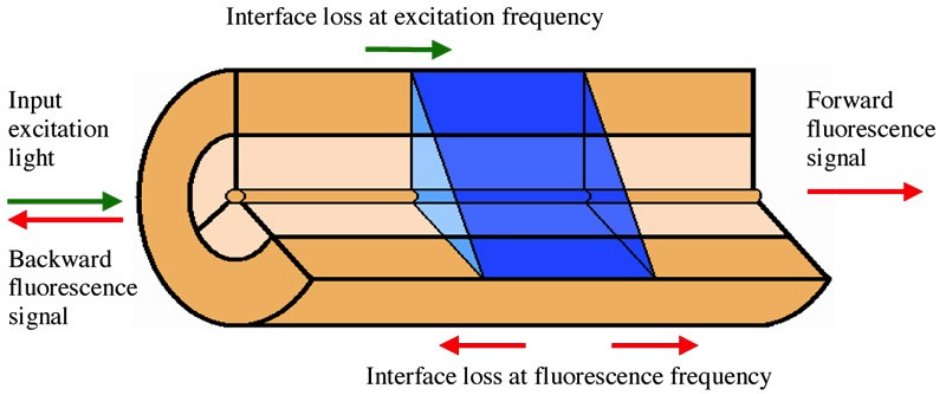

Figure 6: Schematic from Ref. 13 of an EC-MOF with a section immersed in a liquid. Liquid interface losses exist for the excitation light entering the liquid filled section and for the fluorescence exiting the liquid filled section.

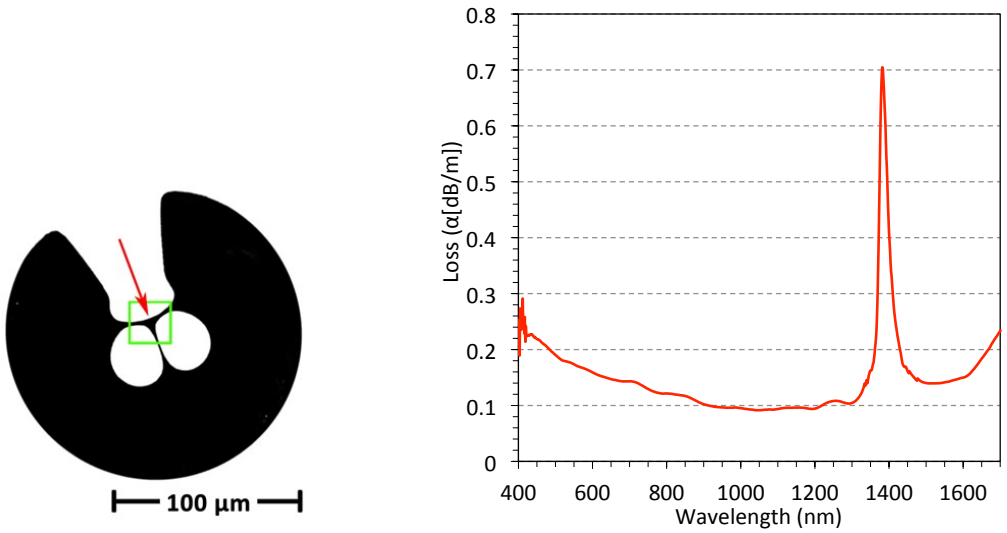

(a) (b)

Figure 7: (a) Contrast enhanced SEM image of (silica material shown in black) EC-MOF cross section, having an effective core diameter of 7.5 μm (core location shown by ▮ – green box) and 160 μm outside diameter; and (b) loss (cutback) measurement of this fiber.

for premixing 8-HQ with the sample are not well suited for real-time, in situ, and/or remote sensing within a fuselage. For such applications it is necessary to immobilize sensor molecules on the glass surface of the EC-MOF exposed core, which can then be used directly as a sensing element without requiring prior pre-mixing of a sample with the sensor molecules. Functionalization methods traditionally used include silanes[18,40] or polyelectrolytes,[41,42] which provide a functional group on the surface to which the sensor molecules can be covalently attached. These processes require several steps that typically take many hours to perform, due to the incubation times needed to achieve consistent maximized binding efficiency.[40,42] Also, results are highly dependent on experimental conditions (temperature, concentration, solvents, hydration and reaction time) as well as pre- and post-treatment processes.[16,19,42,43] These factors can diminish sensor performance, reducing the achievable light-matter interactions, which in turn decreases sensitivity. Apart from these potential difficulties, it

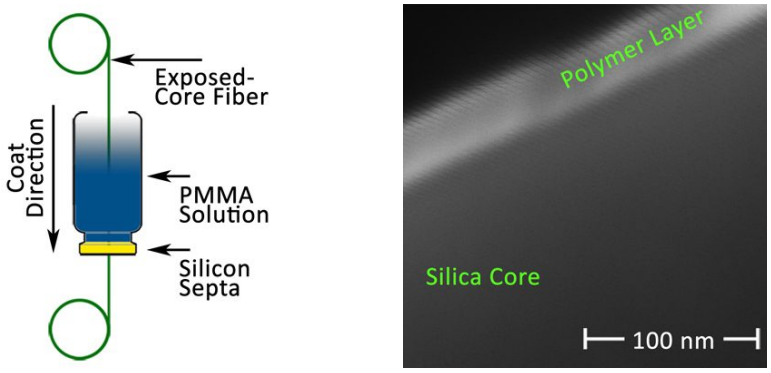

(a) (b)

Figure 8: (a) A schematic of the thin-film polymer coating method used to coat the outside of the MOF including the exposed core region. (b) Close-up SEM of the outside edge of the exposed core (▮ – red arrow in Fig. 7(a)) with 50 nm polymer coating (light grey).

was found that when sensing molecules were covalently attached to the exposed core of a EC-MOF the ability for multiligand binding was negated, although single-ligand binding was still achievable.[44] As an alternative method where the sensing molecule is not covalently bound to the surface, a method of functionalizing EC-MOFs was developed by the authors using a thin film (∼50 nm) PMMA doped with 8-HQ in free form for Al^{3+} detection.[45] This also has the potential to solve some of the practical issues[38] involved in packaging an exposed-core MOF so that it is sensitive to the chosen analyte but protected from the applied sensing environment without the need for surface attachment functional groups.

The method used to functionalize the silica EC-MOFs with thin film PMMA is an extension of the method used for micron scale polymer coating in glass capillaries.[46] A clear cast acrylic rod (PMMA) with a density of 1.18 g/cm^3, also known as a 'plexiglass rod' (Professional Plastics Pte. Ltd. [Singapore]), was dissolved in dichloromethane (DCM) at a concentration of 12.3 g/L. 8-HQ was dissolved in DCM and added to the dissolved PMMA solution making a concentration of $30_{(8\text{-HQ})} : 100_{(\text{PMMA})}$ by weight. One end of the fabricated[37] silica EC-MOF (Fig. 7(a)), with an effective core diameter of 7.5 μm (defined as the diameter of a circle whose area is equal to a triangle that fits wholly within the core area[47]), was fed through a silicon septa fitted to the bottom of an open-end vial. This setup, shown by the schematic in Fig. 8(a), was then used to coat the outside of the EC-MOF including the exposed core region. The PMMA+8-HQ DCM solution was placed into the vial (∼5 mm depth), and the fiber was pulled through the solution and silicon septa by hand (at ∼8 m/min) to leave behind a ∼50 nm coating of the doped PMMA on the core surface (Fig. 8(b)). Uniformity of the polymer layer is critically important for optical performance of the device. Measured results from SEM images of six samples, from the center and 10 cm in from the ends of two individually coated 1 m lengths of fiber, showed the coating thickness on the outside edge of the exposed-core to be in the range 43–46 nm with measurement uncertainty of ±9 nm. The coating procedure was performed in a laboratory chemical fume hood at room temperature (∼21°C), without additional curing.

The impact of deterioration on the transmission properties of the functionalized fiber, resulting from exposing the functionalized fiber to air, was measured using the same procedure detailed in Ref. 38, and briefly described here. A 4 m long PMMA+8-HQ functionalized fiber was coupled to a 100 W halogen broadband source with an approximately Gaussian-distributed intensity profile and peak power at 800 nm. At the other end, the light from the core was imaged onto the detector of an Ando AQ6315E optical spectrum analyzer and the transmitted power spectrum, in dBm, was recorded from 350–1750 nm every two minutes. This procedure was performed in a

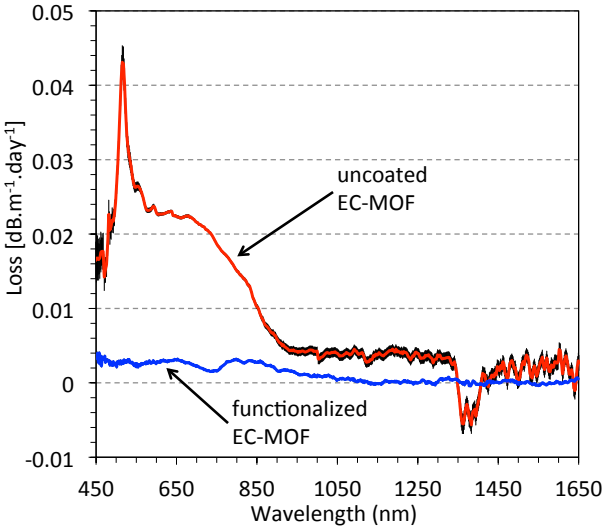

Figure 9: Deterioration in the transmission properties of the air exposed uncoated (▮ – red), from Ref. 38 with 10 μm core diameter) and thin-film polymer functionalized (▮ – blue) silica EC-MOFs. The 95% confidence interval is shown in black. For the thin-film polymer functionalized fiber result, the confidence interval is approximately the same as the line thickness.

laboratory at room temperature (∼21°C), with the fiber in air. This setup was first left long enough (∼6 hours) so that the measured power stabilized to within ±0.05 dBm, then used to take time based measurements of the power for 180 hours. Any changes over time (t) in the transmission characteristics were then fitted to the equation,

$$P(\lambda, t) = P(\lambda, 0)10^{-\xi t z/10} \tag{1}$$

where ξ is the loss in dB $m^{-1}day^{-1}$ and z is the fiber length in meters. For comparison the result in Ref. 38 for an uncoated EC-MOF, with 10 μm core diameter, is shown by the red line in Fig. 9. The result of $\xi(\lambda)$ (Eq. (1)) for the thin-film functionalized fiber, shown by the blue line in Fig. 9, shows a significant improvement compared to the uncoated fiber.

The deterioration in the transmission properties is expected to come from changes in the mechanical and/or compositional characteristics at the core surface, causing light scattering effects.[48–50] When the core diameter is reduced these light scattering effects are expected to increase, as a greater portion of guided light travels outside the core (increased PF). However, this result shows less deterioration in transmission properties even though the core diameter of this functionalized fiber is smaller (7.5 μm) compared to the uncoated EC-MOF from Ref. 38 (10 μm). This shows that the thin film coating is providing a protective function for the core surface. For example, at $\lambda = 532$ nm the air induced deterioration in the transmission properties of the thin-film functionalized fiber (3×10^{-3} dB $m^{-1}day^{-1}$) is an order of magnitude better than for the uncoated result and ∼3 orders of magnitude better than for the previously reported EC-MOFs produced in F2 soft glass.[38] This is significant for optical fiber sensors requiring long term exposure to harsh environmental conditions, such as structural corrosion detection. Further details and results showing the characterization of thin film polymer functionalization layer can be found in Ref. 45.

4. SENSING CORROSION

Measurements were performed to test the ability of the EC-MOF coated with the doped PMMA to detect Al^{3+}. The experimental setup of these measurements is shown in Fig. 10, which consisted of a 405 nm wavelength laser excitation light source coupled to the functionalized EC-MOF. The back reflected light collected from the core of the coated fiber was imaged using a 60× objective, passing through the dichroic mirror and 405 nm Raman long pass filter and 10× objective, and characterized using a Horiba iHR320 Imaging Spectrometer with Synapse CCD Detector. Each measurement was done with a 50 ms pulse of light from the laser. Two separate experiments were performed using this setup, the first of which was to immerse a section of the EC-MOF in a solution containing Al^{3+} and the second experiment used a second section of EC-MOF in a corroded simulated aluminum aircraft joint. For consistency, one longer length of EC-MOF was coated and then cut, with half used on each of the experiments.

For the first experiment the exposed-core region of the coupled EC-MOF was exposed to Al^{3+} by immersing a 23 cm long central section of the fiber in a saturated solution of potassium aluminum sulfate in a capillary. The back reflected spectra were measured before immersion, immediately after immersion and periodically over a 2 hour period. The measured result before immersion subtracted from the after immersion results is presented

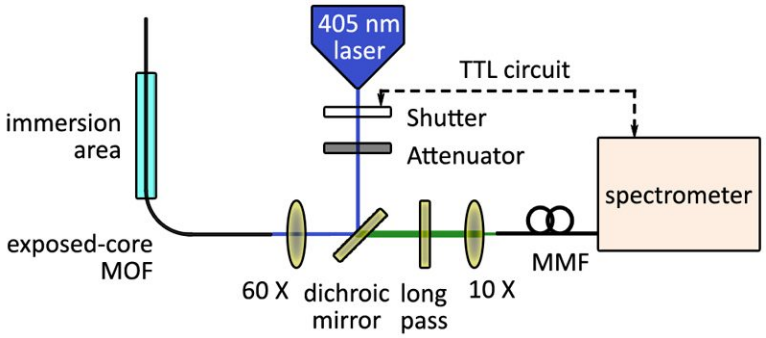

Figure 10: Setup used to test the ability of the coated EC-MOF to detect Al^{3+}.

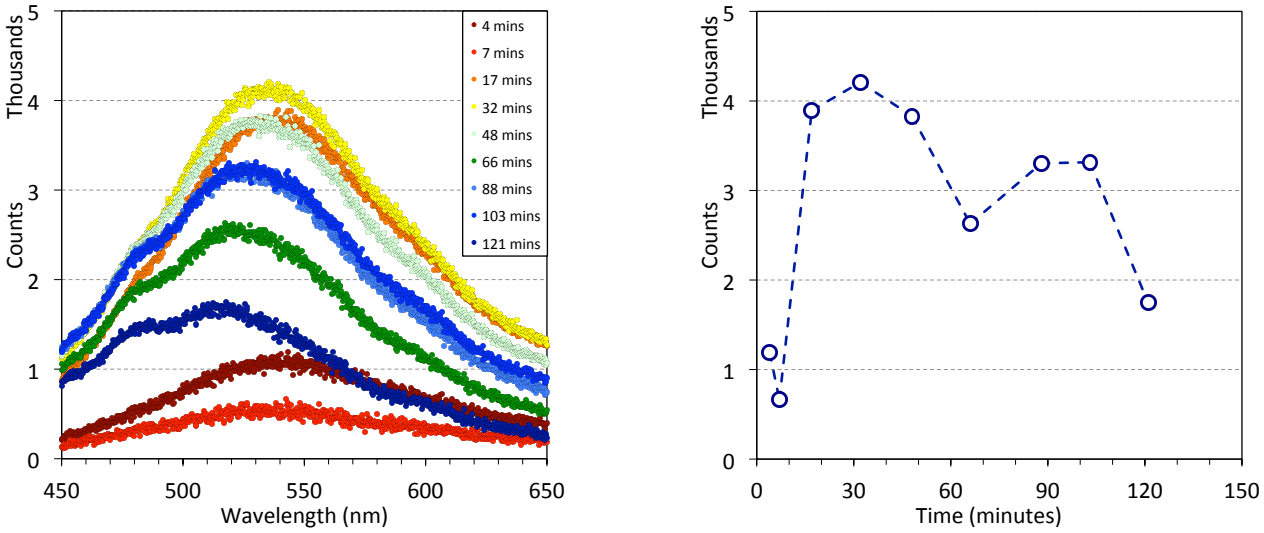

(a) (b)

Figure 11: (a) Periodic measurements of the back reflected spectra of the functionalized fiber immersed in solution containing Al^{3+}, and (b) plot of the peak intensities from the measurements shown in Fig. 11(a) as a function of time.

in Fig. 11(a), which shows the fluorescence peaks of 8-HQ–Al^{3+} complex[10] for a series of immersion times. These in solution measurements demonstrates the ability of the thin polymer film functionalized fiber to detect Al^{3+}. However, over time the measurement deteriorated after peaking around half an hour after immersion, as shown by a plot of the peak intensities as a function of time in Fig. 11(b). The cause of this deterioration was not known, however it may be that the drying saturated solution causes salt crystal formation on the core at the air-liquid interface where the fiber enters and exits the solution.

For the second experiment, a 21 cm long aerospace grade aluminum plate was machined with 2 mm slots and covered with a top plate of 1 cm thick perspex to allow visualization of the corrosion. The perspex was drilled with 2 mm holes along the location of the slots so as to allow the ingress of the corrosive atmosphere to the aluminum. The plate was placed in the highly corrosive atmosphere of a salt spray chamber for four days to induce accelerated corrosion of the aluminum. The corroded plate, shown in Fig. 12(a) was allowed to dry and then the functionalized EC-MOF was placed inside one of the corroded slots, as shown in Fig. 12(b). For a

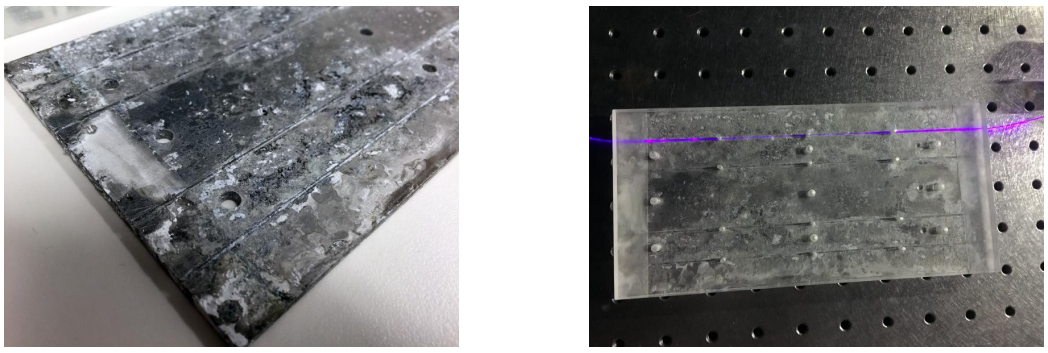

(a) (b)

Figure 12: (a) Aerospace grade aluminum plate after four days in the highly corrosive atmosphere of a salt spray chamber. (b) The corroded plate with a functionalized EC-MOF (▮ – purple) inside one of the slots.

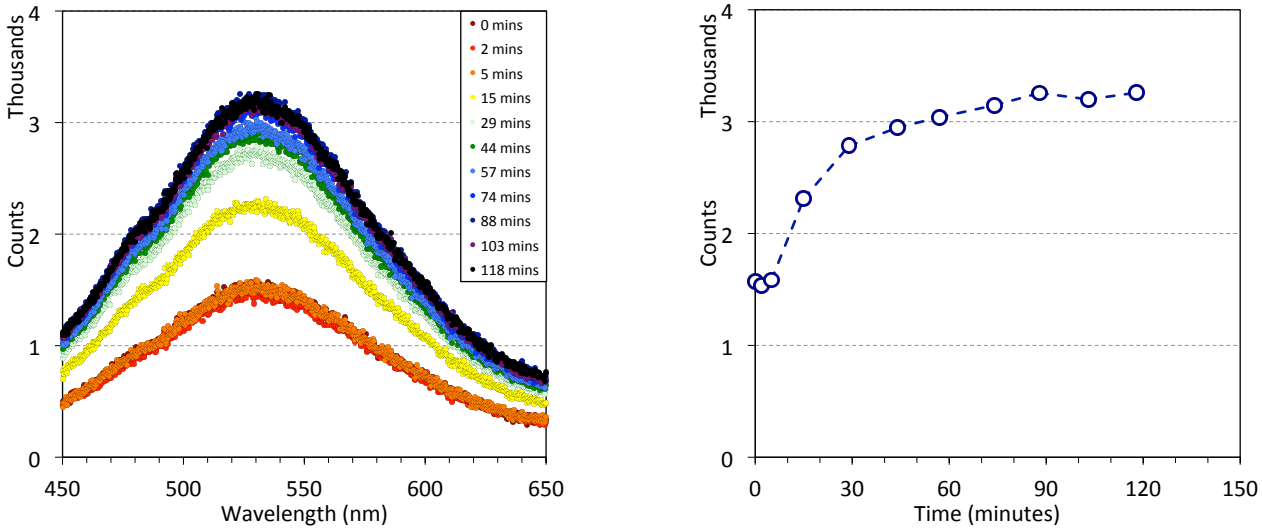

(a) (b)

Figure 13: (a) Periodic measurements of the back reflected spectra of the functionalized fiber inside a corroded simulated aluminum aircraft joint, and (b) plot of the peak intensities from the measurements shown in Fig. 13(a) as a function of time.

background measurement, the back reflected spectra from the EC-MOF was measured while the plate was dry. The slot of the aluminum plate with the fiber inside was then filled with high purity MilliQ water and the back reflected spectra measured immediately and again periodically over a 2 hour period.

The measured results with background subtracted are presented in Fig. 13(a), which shows the fluorescence peaks of 8-HQ–Al^{3+} complex[10] for a series of time intervals after addition of the water. These simulated aluminum aircraft joint measurements demonstrate the ability of the EC-MOF functionalized with a thin polymer film to detect Al^{3+} as a byproduct of corrosion. Figure 13(b) is a plot of the peak intensities of these in plate measurements as a function of time, which shows that there was an immediate initial response from the functionalized fiber which then logarithmically increased over the two hour period.

5. CONCLUSION AND FUTURE WORK

We have summarized progress in the development of a fiber optic detection and monitoring system for corrosion, and have shown that functionalized EC-MOFs can detect Al^{3+} in a simulated aircraft joint. It has been shown in Ref. 51 that the silica EC-MOF fibers can be spliced to single mode fiber for improved handling and integration with commercial interrogation units. Methods are under development to fully connectorize the EC-MOF into a system which incorporates the interrogation and detection instrumentation for use as a field-portable demonstrator. Further work is also required to incorporate a distributed sensing capability so that the position where corrosion is occurring along the length of fiber can be located.

ACKNOWLEDGMENTS

The authors acknowledge support from the Centre for Nanoscale Biophotonics, through Australian Research Council (ARC) CE140100003 and the Australian Defence Science and Technology Group for support under the Strategic Research Initiative Program. The authors acknowledge Peter Henry and Alastair Dowler for their contribution to the silica fiber drawing, Kristopher Rowland and Sabrina Heng for helpful discussions, and Adelaide Microscopy for micrograph support. This work was performed in part at the OptoFab node of the Australian National Fabrication Facility, which provides nano and microfabrication facilities for Australias researchers, utilizing Commonwealth and South Australian State Government funding. Tanya Monro acknowledges the support of an ARC Georgina Sweet Laureate Fellowship.

REFERENCES

[1] Lohner, H. and Hack, T., [*Aluminium Alloy Corrosion of Aircraft Structures: Modelling and Simulation*], WIT Press (2013).

[2] Broomfield, J. et al., "The strategic highway research program. Research on corrosion of steel in concrete.," *P. I. Civil Eng. – Str. B.* **104**(2), 211 – 218 (1994).

[3] McAdam, G., Newman, P. J., McKenzie, I., Davis, C., and Hinton, B. R. W., "Fiber optic sensors for detection of corrosion within aircraft," *Struct. Health Monit.* **4**, 47 – 56 (March 2005).

[4] Warren-Smith, S. C., *Fluorescence-Based Chemical Sensing Using Suspended-Core Microstructured Optical Fibres*, PhD thesis, The University of Adelaide (Oct 2010).

[5] Hall, J., "Corrosion prevention and control programs for boeing airplanes," Technical Paper 931259, SAE International (1993).

[6] Australian Government, "Corrosion prevention and control program (CPCP)," Civil Aviation Safety Regulations 1998 Part 39.001(1), AD/B737/52 Amdt 3, Infrastructure and Regional Development (2011).

[7] McKenzie, I. and Newman, P. J., "Methods for detection of corrosion in aircraft structures using fiber optic technology," in [*Tri-Service Corrosion Conference [15–19 Nov., Myrtle Beach, South Carolina]*], (Nov 1999).

[8] Ščančar, J. and Milačič, R., "Aluminium speciation in environmental samples: a review," *Anal. Bioanal. Chem.* **386**(4), 999 – 1012 (2006).

[9] Shar, G. A. and Soomro, G. A., "8-hydroxyquinoline as a complexing reagent for the determination of Cd(II) in micellar medium," *J. Chem. Soc. Pak.* **27**(5), 471 – 475 (2005).

[10] Kishore, V. V. N. R., Aziz, A., Narasimhan, K. L., Periasamy, N., Meenakshi, P. S., and Wategaonkar, S., "On the assignment of the absorption bands in the optical spectrum of Alq3," *Synthetic Met.* **126**(2–3), 199 – 205 (2002).

[11] Sinchenko, E., Gibbs, W. E. K., Davis, C. E., and Stoddart, P. R., "Characterization of time-resolved fluorescence response measurements for distributed optical-fiber sensing," *Appl. Opt.* **49**, 6385–6390 (Nov 2010).

[12] Schartner, E. P., Ebendorff-Heidepriem, H., Warren-Smith, S. C., White, R. T., and Monro, T. M., "Driving down the detection limit in microstructured fiber-based chemical dip sensors," *Sensors* **11**(3), 2961 – 2971 (2011).

[13] Warren-Smith, S. C., Afshar V., S., and Monro, T. M., "Theoretical study of liquid-immersed exposed-core microstructured optical fibers for sensing," *Opt. Express* **16**, 9034 – 9045 (Jun 2008).

[14] Tong, L., Gattass, R. R., Ashcom, J. B., He, S., Lou, J., Shen, M., Maxwell, I., and Mazur, E., "Subwavelength-diameter silica wires for low-loss optical wave guiding," *Nature* **426**, 816 – 819 (Dec 2003).

[15] Monro, T. M. and Ebendorff-Heidepriem, H., "Progress in microstructured optical fibers," *Annu. Rev. Mater. Res.* **36**(1), 467 – 495 (2006).

[16] Monro, T. M., Warren-Smith, S., Schartner, E. P., François, A., Heng, S., Ebendorff-Heidepriem, H., and Afshar V., S., "Sensing with suspended-core optical fibers," *Opt. Fiber Technol.* **16**(6), 343 – 356 (2010).

[17] Schartner, E. P., Tsiminis, G., François, A., Kostecki, R., Warren-Smith, S. C., Nguyen, L. V., Heng, S., Reynolds, T., Klantsataya, E., Rowland, K. J., Abell, A. D., Ebendorff-Heidepriem, H., and Monro, T. M., "Taming the light in microstructured optical fibers for sensing," *Int. J. Appl. Glass Sci.* **6**(3), 229 – 239 (2015).

[18] Heng, S., Nguyen, M.-C., Kostecki, R., Monro, T. M., and Abell, A. D., "Nanoliter-scale, regenerable ion sensor: sensing with a surface functionalized microstructured optical fibre," *RSC Adv.* **3**, 8308 – 8317 (2013).

[19] Warren-Smith, S. C., Heng, S., Ebendorff-Heidepriem, H., Abell, A. D., and Monro, T. M., "Fluorescence-based aluminum ion sensing using a surface-functionalized microstructured optical fiber," *Langmuir* **27**(9), 5680 – 5685 (2011).

[20] Webb, A. S., Poletti, F., Richardson, D. J., and Sahu, J. K., "Suspended-core holey fiber for evanescent-field sensing," *Opt. Eng.* **46** (Jan 2007).

[21] Euser, T. G., Chen, J. S. Y., Scharrer, M., Russell, P. S. J., Farrer, N. J., and Sadler, P. J., "Quantitative broadband chemical sensing in air-suspended solid-core fibers," *J. Appl. Phys.* **103**(10), 103108 (2008).

[22] Mazhorova, A., Markov, A., Ng, A., Chinnappan, R., Skorobogata, O., Zourob, M., and Skorobogatiy, M., "Label-free bacteria detection using evanescent mode of a suspended core terahertz fiber," *Opt. Express* **20**, 5344–5355 (Feb 2012).

[23] Afshar V., S., Warren-Smith, S. C., and Monro, T. M., "Enhancement of fluorescence-based sensing using microstructured optical fibres," *Opt. Express* **15**, 17891 – 17901 (Dec 2007).

[24] Ruan, Y., Schartner, E. P., Ebendorff-Heidepriem, H., Hoffmann, P., and Monro, T. M., "Detection of quantum-dot labelled proteins using soft glass microstructured optical fibers," *Opt. Express* **15**, 17819 – 17826 (Dec 2007).

[25] Cox, F. M., Lwin, R., Large, M. C. J., and Cordeiro, C. M. B., "Opening up optical fibres," *Opt. Express* **15**, 11843–11848 (Sep 2007).

[26] Warren-Smith, S. C., Ebendorff-Heidepriem, H., Foo, T. C., Moore, R., Davis, C., and Monro, T. M., "Exposed-core microstructured optical fibers for real-time fluorescence sensing," *Opt. Express* **17**, 18533 – 18542 (Oct 2009).

[27] Afshar V., S., Ruan, Y., Warren-Smith, S. C., and Monro, T. M., "Enhanced fluorescence sensing using microstructured optical fibers: a comparison of forward and backward collection modes," *Opt. Lett.* **33**, 1473 – 1475 (Jul 2008).

[28] Warren-Smith, S. C., Sinchenko, E., Stoddart, P. R., and Monro, T. M., "Distributed fluorescence sensing using exposed core microstructured optical fiber," *IEEE Photon. Technol. Lett.* **22**, 1385 – 1387 (Sep 2010).

[29] Warren-Smith, S. C., Ebendorff-Heidepriem, H., Afshar V., S., McAdam, G., Davis, C., and Monro, T., "Corrosion sensing of aluminium alloys using exposed-core microstructured optical fibres," *Mater. Forum* **33**, 110 – 121 (2009).

[30] Richardson, K., Krol, D., and Hirao, K., "Glasses for photonic applications," *Int. J. Appl. Glass Sci.* **1**(1), 74 – 86 (2010).

[31] Peters, K., "Polymer optical fiber sensors - a review," *Smart Mater. Struct.* **20**(1), 013002 (2011).

[32] Law, S. H., van Eijkelenborg, M. A., Barton, G. W., Yan, C., Lwin, R., and Gan, J., "Cleaved end-face quality of microstructured polymer optical fibres," *Opt. Commun.* **265**(2), 513 – 520 (2006).

[33] Atakaramians, S., Cook, K., Ebendorff-Heidepriem, H., Afshar V., S., Canning, J., Abbott, D., and Monro, T. M., "Cleaving of extremely porous polymer fibers," *IEEE Photon. J.* **1**, 286 – 292 (Dec 2009).

[34] Stefani, A., Nielsen, K., Rasmussen, H. K., and Bang, O., "Cleaving of TOPAS and PMMA microstructured polymer optical fibers: Core-shift and statistical quality optimization," *Opt. Commun.* **285**(7), 1825 – 1833 (2012).

[35] Li, M. and Nolan, D. A., "Optical transmission fiber design evolution," *J. Lightwave Technol.* **26**(9), 1079 – 1092 (2008).

[36] Heraeus Quarzglas GmbH & Co. KG, http://heraeus-quarzglas.com/, *Pure Silica Rods for Specialty Fiber Applications*, 1st edition ed. (Jan 2012).

[37] Kostecki, R., Ebendorff-Heidepriem, H., Warren-Smith, S. C., and Monro, T. M., "Predicting the drawing conditions for microstructured optical fiber fabrication," *Opt. Mater. Express* **4**, 29 – 40 (Jan 2014).

[38] Kostecki, R., Ebendorff-Heidepriem, H., Davis, C., McAdam, G., Warren-Smith, S. C., and Monro, T. M., "Silica exposed-core microstructured optical fibers," *Opt. Mater. Express* **2**, 1538 – 1547 (Nov 2012).

[39] Lodeiro, C., Capelo, J. L., Mejuto, J. C., Oliveira, E., Santos, H. M., Pedras, B., and Nunez, C., "Light and colour as analytical detection tools: A journey into the periodic table using polyamines to bio-inspired systems as chemosensors," *Chem. Soc. Rev.* **39**, 2948 – 2976 (2010).

[40] Foo, H. T. C., Ebendorff-Heidepriem, H., Sumby, C. J., and Monro, T. M., "Towards microstructured optical fibre sensors: Surface analysis of silanised lead silicate glass," *J. Mater. Chem. C* **1**, 6782 – 6789 (2013).

[41] Sciacca, B., François, A., Klingler-Hoffmann, M., Brazzatti, J., Penno, M., Hoffmann, P., and Monro, T. M., "Radiative-surface plasmon resonance for the detection of apolipoprotein E in medical diagnostics applications," *Nanomed. - NBM* **9**(4), 550 – 557 (2013).

[42] François, A., Ebendorff-Heidepriem, H., Sumby, C. J., and Monro, T. M., "Comparison of surface functionalization processes for optical fibre biosensing applications," in [*20th International Conference on Optical Fibre Sensors*], *Proc. SPIE* **7503** (2009).

[43] Zhu, M., Lerum, M. Z., and Chen, W., "How to prepare reproducible, homogeneous, and hydrolytically stable aminosilane-derived layers on silica," *Langmuir* **28**(1), 416 – 423 (2012).

[44] Kostecki, R., Heng, S., Ebendorff-Heidepriem, H., Abell, A. D., and Monro, T. M., "Functionalization of exposed core fibers with multiligand binding molecules for fluorescence based ion sensing," in [*23rd International Conference on Optical Fibre Sensors*], *Proc. SPIE* **9157** (2014).

[45] Kostecki, R., Ebendorff-Heidepriem, H., Afshar V., S., McAdam, G., Davis, C., and Monro, T. M., "A novel polymer functionalization method for exposed-core optical fiber," *Opt. Mater. Express* **4**, 1515 – 1525 (Aug. 2014).

[46] Rowland, K. J., François, A., Hoffmann, P., and Monro, T. M., "Fluorescent polymer coated capillaries as optofluidic refractometric sensors," *Opt. Express* **21**, 11492 – 11505 (May 2013).

[47] Ebendorff-Heidepriem, H., Warren-Smith, S. C., and Monro, T. M., "Suspended nanowires: fabrication, design and characterization of fibers with nanoscale cores," *Opt. Express* **17**, 2646 – 2657 (Feb 2009).

[48] Brambilla, G., Xu, F., and Feng, X., "Fabrication of optical fibre nanowires and their optical and mechanical characterisation," *Electron. Lett.* **42**, 517 – 519 (april 2006).

[49] Zhai, G. and Tong, L., "Roughness-induced radiation losses in optical micro or nanofibers," *Opt. Express* **15**, 13805 – 13816 (Oct 2007).

[50] Fujiwara, M., Toubaru, K., and Takeuchi, S., "Optical transmittance degradation in tapered fibers," *Opt. Express* **19**, 8596 – 8601 (Apr 2011).

[51] Warren-Smith, S. C., Kostecki, R., Nguyen, L. V., and Monro, T. M., "Fabrication, splicing, bragg grating writing, and polyelectrolyte functionalization of exposed-core microstructured optical fibers," *Opt. Express* **22**(24), 29493 – 29504 (2014).